Journal of Sound and Vibration (1998) **210**(1), 137–152

FORMULATION, IMPLEMENTATION AND VALIDATION OF MULTIPLE CONNECTION AND FREE EDGE CONSTRAINTS IN AN INDIRECT BOUNDARY ELEMENT FORMULATION

N. VLAHOPOULOS

Department of Naval Architecture and Marine Engineering, *The University of Michigan*, 2600 *Draper Road*, 214 *NAME Bldg*., *Ann Arbor*, *MI* 48109-2145, *U.S.A*.

AND

S. T. RAVEENDRA

Automated Analysis Corporation, 2805 *S. Industrial*, *Suite* 100, *Ann Arbor*, *MI* 48104-6767, *U.S.A*.

(*Received* 18 *December* 1996, *and in final form* 5 *September* 1997)

The Indirect Boundary Element Method (IBEM) can be used in numerical simulations for computing the noise radiated from vibrating structures or the combined structural acoustic response of a system. The primary variable on the surface of the model is defined as the difference in the pressure between its two sides. When the boundary element model contains multiple elements connected along the same edge or openings, then the definition of the primary variables must be adapted in order to reflect the complexity of the geometry. In order to accommodate the new definitions, the connectivity of the boundary element model must be updated and constraint equations must be generated and introduced in the boundary element system of equations. Special attention is required when multiple connections and free edges occur in the same physical location. This work presents a mathematical formulation associated with the multiple connection and the free edge constraints, its numerical implementation, an algorithm for the automated update of the boundary element model, and validation of all the developments.

1. INTRODUCTION

The boundary element method has been used extensively in numerical acoustics to compute the noise radiated from vibrating objects, the noise generated inside acoustics cavities from panel vibration, or to solve noise diffraction problems [1]. It is based on expressing the acoustic variables (pressure, velocity, intensity) within the acoustic volume as a surface integral over the boundary of the acoustic domain. The surface integral contains the primary variables of the formulation, the Green's function, and derivatives of it. There are two distinct boundary element formulations available, the direct (DBEM) and the indirect (IBEM). The difference between them stems from the definition of the primary variables. The acoustic pressure and the acoustic velocity are the primary variables defined in the direct method [2–4]. The difference in the pressure and the differene in the normal gradient of the pressure are the primary variables utilized in the indirect method [5–7]. In the direct method, there is a distinction between an interior or an exterior analysis

0022–460X/98/060137 + 16 $25.00/0/sv971299

depending on whether the primary variables are defined on the interior or exterior side of the model. In the indirect method there is no such differentiation. The formulation is developed by accounting for the acoustic medium on both sides of the model as will be explained in section 2, therefore the primary variables contain information from the interior and the exterior acoustic space. The indirect formulation can be combined with a variational approach [8] in deriving the primary system of equations. Then by taking into account the boundary conditions a numerical solution can be produced. The attractive feature of such an approach is that the boundary element system of equations is symmetric. It therefore requires reduced computer resources for assembly and solution. Further, an indirect boundary element model can include openings and multiple connections (Figure 1). This is possible because the definition of the primary variables accounts for the acoustic medium on both sides. There are two issues associated with modelling these geometric complexities. At a free edge of an opening the acoustic pressure is the same for both sides of the model and that must be accounted for properly when defining the primary variables at the nodes residing along the free edge. Further, along the common edge of a multiple connection, the number of the defined acoustic sub-spaces equals the number of panels connected along the same edge. This creates an inconsistency in the definition of the primary variables as explained in section 2. The algorithm developed in this work addresses these issues.

For each type of constraint (free edge or multiple connection), work has been done in three areas: (1) Expressing the physical implication of a free edge or a multiple connection constraint in terms of a mathematical formulation. (2) Imposing the constraints in the numerical system of equations associated with the boundary element formulation. (3) Identifying the nodes where a constraint must be applied and updating the model to accommodate the mathematical and numerical definition of the constraints.

The capability of modelling free edges and multiple connections is important in industrial applications such as engine enclosures, powertrain models [9], intake and exhaust systems [10], heavy equipment cabs [11] and automotive compartments [12, 13].

2. MATHEMATICAL BACKGROUND FOR THE INDIRECT BOUNDARY ELEMENT METHOD

A brief mathematical background information on the IBEM will be given in this section. It will allow us to identify how the definition of the primary variables is associated with the mathematical formulation and the numerical implementation of the free edge and the

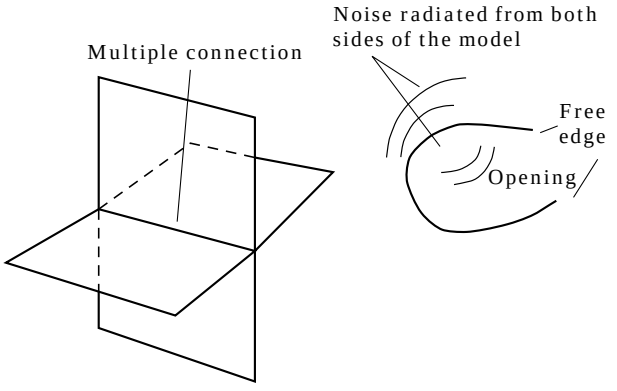

Figure 1. Simple models demonstrating a multiple connection and an opening.

multiple connection constraints. The development work presented here is based on this relationship.

The boundary element method is based on expressing the acoustic pressure at a point within the acoustic medium as an integral over the boundary defining the acoustic domain. This is known as the Helmholtz integral equation [1–3, 14],

$$Cp(\mathbf{r}_{dr}) = \int_s G(\mathbf{r}, \mathbf{r}_{dr}) \frac{\partial p(\mathbf{r})}{\partial n} - \frac{\partial G(\mathbf{r}, \mathbf{r}_{dr})}{\partial n} p(\mathbf{r}) \, \mathrm{d}s, \tag{1}$$

where $\mathbf{r}$ is the point vector on the surface of the boundary element model, G denotes Green's function, $\mathbf{r}_{dr}$ is the vector specifying the location of the data recovery point, $p(\mathbf{r}_{dr})$ is the acoustic pressure at location $\mathbf{r}_{dr}$ and C is the integration constant resulting from the integration of Dirac's function originating from the fundamental solution to the governing differential wave equation. The acoustic variables $p(\mathbf{r})$ and $\partial p(\mathbf{r})/\partial n$ on the surface of the boundary element model are located either on the interior or exterior side of the boundary element model.

In order to derive the integral equation for the indirect formulation the standard approach used in indirect boundary element formulations [15, 16] is applied. The integral equations for the two acoustic spaces are added together. Within the integral the terms which include Green's function are factored out and the opposite direction of the unit normal between the two equations is taken into account in generating the new primary variables. The equations for the primary variables and the acoustic pressure at a data recovery point are (equations (2) and (3), respectively):

$$\delta p = p_1 - p_2, \qquad \delta \mathrm{d}p = \left(\frac{\partial p}{\partial n}\right)_1 - \left(\frac{\partial p}{\partial n}\right)_2, \tag{2}$$

$$p(\mathbf{r}_{dr}) = \int_{s_a} \delta p(\mathbf{r}_a) \frac{\partial G(\mathbf{r}_a, \mathbf{r}_{dr})}{\partial n_a} - G(\mathbf{r}_a, \mathbf{r}_{dr}) \delta \mathrm{d}p(\mathbf{r}_a) \, \mathrm{d}S(\mathbf{r}_a), \tag{3}$$

where δp is the difference in pressure between the two sides of the boundary ("δ" indicates the difference), and $\delta \mathrm{d}p$ is the difference in the normal gradient of the pressure ("δ" indicates the difference and "d" indicates the differentiation).

From the boundary conditions either one of the primary variables is specified, or a relationship between them can be derived. In areas of the boundary with pressure boundary condition, $\delta \mathrm{d}p$ becomes the unknown variable, while in areas of the boundary with velocity or impedance boundary condition, δp comprises the unknown variable. In this work, velocity or impedance boundary conditions are considered in the areas where either free edges or multiple connections can be encountered. This is valid because in a physical system, a prescribed pressure boundary condition can only be assigned to simulate the known value of a propagating wave, and multiple connections among propagating waves or free edges do not have any physical substance.

In order to demonstrate how the numerical system of equations is derived, a velocity boundary condition will be assumed. The data recovery point is then positioned on the

boundary element model, and the value of the velocity boundary condition is expressed as an integral of the unknown primary variable δp over the surface of the model:

$$-i\rho\omega v(\mathbf{r}_b) = \int_{S_a} \delta p(\mathbf{r}_a) \frac{\partial^2 G(\mathbf{r}_a, \mathbf{r}_b)}{\partial n_a \partial n_b} \, \mathrm{d}S(\mathbf{r}_a). \tag{4}$$

It is attractive to use a variational approach [8] in deriving the numerical system of equations. There are two reasons for that: computational savings since the system matrix will be symmetric; and the potential of coupling to a symmetric finite element matrix for solving a coupled elasto-acoustic system [6–7]. The variational principal utilized in this solution indicates that the solution to equation (5) will also minimize the functional presented in equation (6):

$$\mathfrak{R}(\phi) - f = 0, \qquad F(\phi) = \int_S \phi \mathfrak{R}(\phi) \, \mathrm{d}S - 2 \int_S \phi f \, \mathrm{d}S, \tag{5, 6}$$

where $\mathfrak{R}(\phi)$ is the operator on function, f is a known function, and $F(\phi)$ is the quadratic functional. In equation (4), $-i\rho\omega v(\mathbf{r}_b)$ corresponds to f of equation (5), and the integral in equation (4) corresponds to the operator $\mathfrak{R}(\phi)$ of equation (5). Therefore the functional is derived as

$$F = 2 \int_{S_b} i\rho\omega v(\mathbf{r}_b) \delta p(\mathbf{r}_b) \, \mathrm{d}S(\mathbf{r}_b) + \int_{S_b} \int_{S_a} \delta p(\mathbf{r}_b) \delta p(\mathbf{r}_a) \frac{\partial^2 G(\mathbf{r}_a, \mathbf{r}_b)}{\partial n_a \partial n_b} \, \mathrm{d}S(\mathbf{r}_a) \, \mathrm{d}S(\mathbf{r}_b). \tag{7}$$

The minimization condition for the functional combined with a numerical discretization of the boundary element model into nodes and elements results in a symmetric system of equations,

$$[A]\{\delta p\} = \{f_v\}, \tag{8}$$

where $\{f_v\}$ is the forcing vector derived from the velocity boundary conditions, $\{\delta p\}$ is the vector containing the unknown primary variables at the nodal locations, and $[A]$ is the symmetric boundary element system of equations. Once equation (8) is solved, the distribution of the primary variables over the surface of the model is determined and the acoustic response can be computed at any data recovery point from equation (3).

3. MATHEMATICAL FORMULATION AND NUMERICAL IMPLEMENTATION OF THE FREE EDGE AND THE MULTIPLE CONNECTION CONSTRAINTS

The presence of a free edge in a boundary element model has to be reflected in the primary system (8). The physical phenomenon along a free edge is the continuity of the acoustic pressure between the acoustic spaces from the two sides of the model. The implication in the primary variables is that the difference in the pressure δp along the free edge has to be zero:

$$\delta p_k = 0, \qquad k = 1, \ldots, K, \tag{9}$$

where δp_k is the nodal value of the primary variable δp on a node along a free edge, and K is the total number of nodes along the free edges in the boundary element model. Therefore, there are two issues associated with the free edge constraints. The first is to identify the nodes on the free edges of a given boundary element model. This is accomplished by the algorithm described in section 4. The second is to enforce the values

of the primary variable δp corresponding to the free edge nodes to become equal to zero during the solution of the primary system of equations. This is achieved by using a penalty method approach. Specifically, if k is one of the nodes on a free edge then in the primary system of equations a penalty term with a large value is added to the corresponding diagonal term:

$$\begin{bmatrix} a_{11} & a_{12} & \cdot\cdot & & \cdot\cdot & a_{1I} \\ & \cdot & \cdot\cdot & & \cdot\cdot & a_{2I} \\ & & \cdot & \cdot & \cdot\cdot & \cdot \\ \text{sym} & & & a_{kk}+PT_k & & a_{kI} \\ & & & & \cdot\cdot & \cdot \\ & & & & & a_{II} \end{bmatrix} \begin{Bmatrix} \delta p_1 \\ \cdot \\ \cdot \\ \delta p_k \\ \cdot \\ \delta p_I \end{Bmatrix} = \begin{Bmatrix} f_1 \\ \cdot \\ \cdot \\ f_k \\ \cdot \\ f_I \end{Bmatrix}, \tag{10}$$

where a_{ij} denotes the entries in the primary system of equations, I is the total number of nodes in the boundary element model, δp_i are the primary variables, f_i is the forcing function associated with the boundary conditions, and PT_K is the penalty term associated with the kth node. It is important to account for the order of magnitude of the terms in the numerical system of equations when using the penalty method. This is achieved by taking a summation of the absolute values of the entries of the row associated with the diagonal term where the penalty term will be imposed:

$$SM_k = \sum_{i=1}^{I} |a_{ki}|. \tag{11}$$

Then the penalty term is assigned the value

$$PT_k = SM_k 10^8. \tag{12}$$

The value of 10^8 is a typical one utilized in numerical applications to enforce a variable in a system of equations to acquire a certain value during solution [17]. When the distribution of the primary variables is computed from equation (10), the variables corresponding to nodes residing on the free edge become zero. This impacts the numerical values derived for the remaining nodes, and it allows us to account for the existence of the free edges in the model. The presence of multiple connections in a boundary element model must also be reflected in the primary system (8). Physically, around a multiple connection, there are as many individual acoustic spaces generated as the number of connecting faces (Figure 2). The challenge for the acoustic formulation is in defining the primary variable δp on the nodes along the common edge of the multiple connection. By definition, δp is equal to the difference in the pressure between the two sides of the model. For the nodes on the multiple connection it is not possible to uniquely define the primary variable since there are more than two acoustic spaces present. In this work this obstacle is alleviated by generating new nodes at the connection; then a unique definition of the primary variables is feasible. In addition, a constraint equation must be developed between the uniquely defined primary variables. It represents their association to each other since they originate from the same common edge. Similar to the free edge constraints, two issues must be resolved in representing the multiple connection constraint in the boundary element system of equation (8). The multiple connections existing in the model must be identified, new nodes must be generated, and the nodal connectivity of the elements must be updated accordingly. This is achieved by the algorithm presented in section 4. The multiple connection must be expressed mathematically as a constraint equation. This is

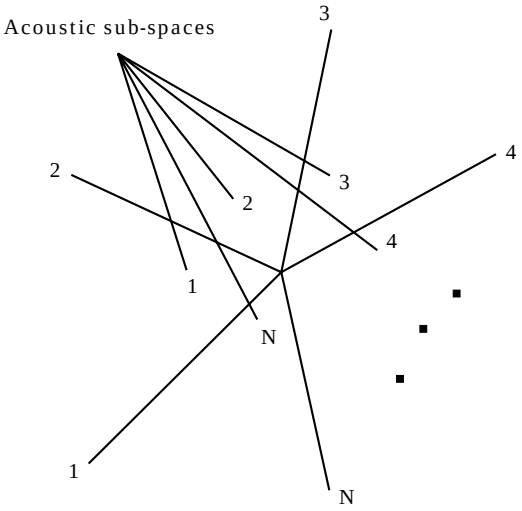

Figure 2. Acoustic spaces around a multiple connection.

achieved by observing the manner in which the variables are defined. For example, the simplest multiple connection is the one where three elements are connected together (Figure 3). The unit normal on each element dictates the definition of the primary variable δp at the nodes of the element. The pressure of the acoustic space towards which the unit normal is pointing is the one included first in the definition of δp. This convention determines the constraint equation which forms the multiple connection constraint. Due to repetition of the acoustic pressure from an acoustic sub-space in the definition of the primary variables between neighboring elements, the primary variables originating from the same node must satisfy the general equation

$$\sum_{n_m=1}^{N_m} c_{n_m} \delta p_{n_m} = 0, \tag{13}$$

where N_m is the total number of nodes participating in the mth multiple connection, n_m is the index associated with the mth constraint, δp_{n_m} is the primary variable on node n_m, and c_{n_m} is the constant corresponding to the n_m primary variable of the mth multiple connection constraint. The value assigned to c_{n_m} depends on the orientation of the

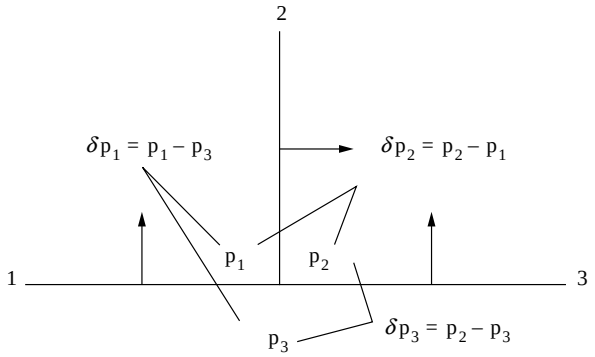

Figure 3. Multiple connection with three elements.

corresponding element. By turning in a clockwise direction around the multiple connection, if the unit normal is along the clockwise direction, then $c_{n_m} = +1$, otherwise $c_{n_m} = -1$. Equation (13) represents the association between the primary variables at the multiple connection. The next step in the mathematical formulation is to impose the condition for equation (13) to the solution vector of the primary system of equation which can be represented as

$$\begin{bmatrix} a_{11} & a_{12} & & a_{1I} \\ & \cdot & & \cdot \\ \text{sym} & & a_{s+n_m,\,s+n_m} & a_{s+n_m,\,I} \\ & & & \cdot \quad \cdot \\ & & & a_{II} \end{bmatrix} \begin{Bmatrix} \delta p_1 \\ \cdot \\ \delta p_{s+n_m} \\ \cdot \\ \delta p_I \end{Bmatrix} = \begin{Bmatrix} f_1 \\ \cdot \\ f_{s+n_m} \\ \cdot \\ f_I \end{Bmatrix}, \tag{14}$$

where index s is the index asociated with the global numbering of the first node in the mth multiple connection constraint. Typically in a boundary element model representing a complex geometry there are several groups of nodes associated with multiple connections ($m = 1, \ldots, M$, where M is the total number of multiple connections). After the solution of the system (14) is completed, the values obtained for each group of primary variables originating from the same node must satisfy equation (13). The Langrange multiplier method [18] is employed in order to impose the multiple connection constraints. The functional F from equation (7), is subject to M constraints,

$$h_m = \sum_{n_m=1}^{N_m} c_{n_m} \delta p_{n_m} = 0, \qquad m = 1, \ldots, M, \tag{15}$$

where h_m is the mth multiple connection constraint equation. The Lagrange multiplier method in this case reduces to extremizing the auxiliary functional

$$F^* = F + \sum_{m=1}^{M} \lambda_m h_m = F + \sum_{m=1}^{M} \lambda_m^* \left(\sum_{n_m=1}^{N_m} c_{n_m} \delta p_{n_m} \right) = 0, \tag{16}$$

where λ_m represents the Lagrange multiplier associated with the mth multiple connection constraint. Then system (14) becomes

$$\begin{bmatrix} a_{11} & a_{12} & & & a_{1\mathrm{I}} & 0 \\ & \cdot & \cdot\cdot & & & \cdot\cdot \\ & & & a_{s+m_n,\,s+m_n} & & \mathrm{c}_{\mathrm{n_m}}\cdot\cdot \\ & & & & \cdot\cdot & \\ \text{sym} & & & & a_{\mathrm{II}} & \\ & & & & & \cdot\cdot \\ & & & & & 0 \end{bmatrix} \begin{Bmatrix} \delta p_1 \\ \cdot \\ \delta p_{s+n_m} \\ \cdot \\ \delta p_I \\ \lambda_1 \\ \cdot \\ \lambda_M \end{Bmatrix} = \begin{Bmatrix} f_1 \\ \cdot \\ \mathrm{f_{s+n_m}} \\ \cdot \\ f_I \\ 0 \\ \cdot \\ 0 \end{Bmatrix}. \tag{17}$$

The size of the system increases by the total number of constraint equations which is equal to

$$\sum_{m=1}^{M} N_m.$$

The concept of multiple connection constraints in the IBEM is similar to the concept of multi-point constraints in structural finite element analysis.

4. AUTOMATED IDENTIFICATION AND GENERATION OF THE FREE EDGE AND MULTIPLE CONNECTION CONSTRAINTS

In order to impose the free edge or the multiple connection constraints to the numerical system of equations, it is necessary to identify the nodes associated with each constraint category. In addition, for multiple connection constraints, additional nodes must be generated and the connectivity of the elements at the connections must be adapted. Also, the value of the c_{n_m} coefficients (equation (13)) must be determined, depending on the relative orientation of the elements at the multiple connection. In this work, the process has been automated and implemented in a computer program. The individual steps comprising the process are summarized as follows. (1) The element side is identified as an entity, and the corresponding element connectivity is created. (2) Nodes on a free edge or on a multiple connection are identified. (3) The elements involved in multiple connections are identified, and the nodes participating in the multiple connection are duplicated. (4) Groups of elements along a continuous side of a multiple connection are formed. (5) Within each group, the nodes participating in the multiple connection are equivalenced for adjacent elements within the group. (6) The constraints are generated as entities. (7) Duplicate constraints which may exist are eliminated. (8) The numbering associated with the valid constraints, and the numbering for the nodes, is compressed. (9) The nodes where the free edge constraints have been assigned are inspected in order to determine whether a multiple connection constraint must also be assigned at the same location, or if some elements must be disassociated from the free edge constraint. (10) The constraint definition is adapted for the nodes identified during the previous step. (11) The information on the free edge and the multiple connection constraints is transferred to the indirect boundary element analysis process.

It is evident that there are several procedures associated with the automated generation of the constraints. The rational behind each one, and its functionality are described below.

The element side is identified as an entity, *and the corresponding element connectivity is created*. A free edge or a multiple connection can be identified depending on how many times a certain element side is shared between different elements. If it is attached to a unique element then a free edge occurs. If the same side is attached to three or more elements then a multiple connection is encountered. In this case the number of elements sharing the same side will dictate the number N_m of the nodes involved in each constraint relationship of equation (13). The two nodes comprising each element side are used to define the entity. The order in which they are defined is not important. The connectivity of an element is presented in terms of its sides in addition to its connectivity based on nodes. This information will be used later in the process of identifying elements involved in multiple connection constraints.

Nodes on a free edge or on a multiple connection are identified. Depending on whether a side is involved in a free edge or in a multiple connection, the nodes of the model are separated into groups. There are three groups of nodes. Those which are associated with a free edge, those which are associated with a multiple connection, and those which are not associated with any constraint. It is important to identify the nodes in the constraints because the constraint equations (equation (9) or equation (13)) are nodal based.

The elements involved in multiple connections are identified, *and the nodes participating in the multiple connection are duplicated*. The elements which have one or more nodes attached to a multiple connection are identified. This is achieved by checking if the nodes

of an element also belong to the group of sides associated with the multiple connections. Each time a node is identified to be on a multiple connection, its number changes to a unique number higher than the total number of nodes in the original model. The connectivity of the element is adapted accordingly. The information of the original node number is also stored for later use.

Groups of elements along a continuous side of a multiple connection are formed. Unique groups of elements, containing all the elements along the same side of a multiple connection are created. This is achieved by first identifying an element which has not been associated with any group. This then comprises the first element of the new group. Elements are inserted in the group by having a common side with any of the other elements already within the group, provided that the common side is not along a multiple connection. When no new elements can become part of the group, then the search for the particular group is terminated. The process is completed when all the elements associated with multiple connection constraints have been inserted into groups.

Within each group the nodes participating in the multiple connection are equivalenced for adjacent elements within the group. During the third step all the nodes on the multiple connection edges had their numbers modified to a higher unique value. This was done in order to create new nodes at the multiple connection locations. However, nodes which originate from the same node, and are attached to adjacent elements of the same group have to be equivalenced. This is accomplished within this step. For every element within a group, the number assigned to its nodes is compared to the highest node number in original model. If the node is higher, it means that this particular node was duplicated during the third step. This indicates that it is one of the nodes which must be potentially equivalenced to nodes of adjacent elements within the same group. Therefore, its original node number is compared against the original node numbers of nodes with the same properties. The coincident nodes are equivalenced by equating all their numbers to the lowest one. The connectivity of the elements to which they are attached is modified accordingly.

The constraints are generated as entities. Prior to the current step the model was adapted leading to the generation of the constraints. The latter are considered as entities comprised by the number of nodes included in each constraint equation, the node numbers, and the directional coefficient c_{n_m} associated with each one of the nodes. For every side entity involved in a multiple connection constraint, the elements which share the same side are identified. Then two constraint entities are generated for each group of nodes associated with the two ends of the side. The orientation of the elements is identified from the order of nodes in the element connectivity. Elements with the same orientation along the common side are assigned the same value for the directional coefficient. Elements with opposite orientation are assigned values of opposite sign. Since in this step two constraint entities are generated for each constraint side, in several instances more than one constraint has been generated for the same group of nodes. This matter is handled in the following step.

Duplicate constraints which may exist are eliminated. Each constraint is compared against all others. If another one is found containing the identical group of nodes, then that one is eliminated as redundant. In this manner all the constraints are associated with a unique group of nodes. This process was selected to be an independent step rather than to take place concurrently with the sixth step for simplicity and reduced computations.

The numbering associated with the valid constraints, *and the numbering for the nodes are compressed*. Since the redundant constraints are eliminated, the number identifying each one of them is compressed in order to achieve a consecutive numbering scheme. Similarly the number assigned to each one of the nodes is compressed to a sequential numbering

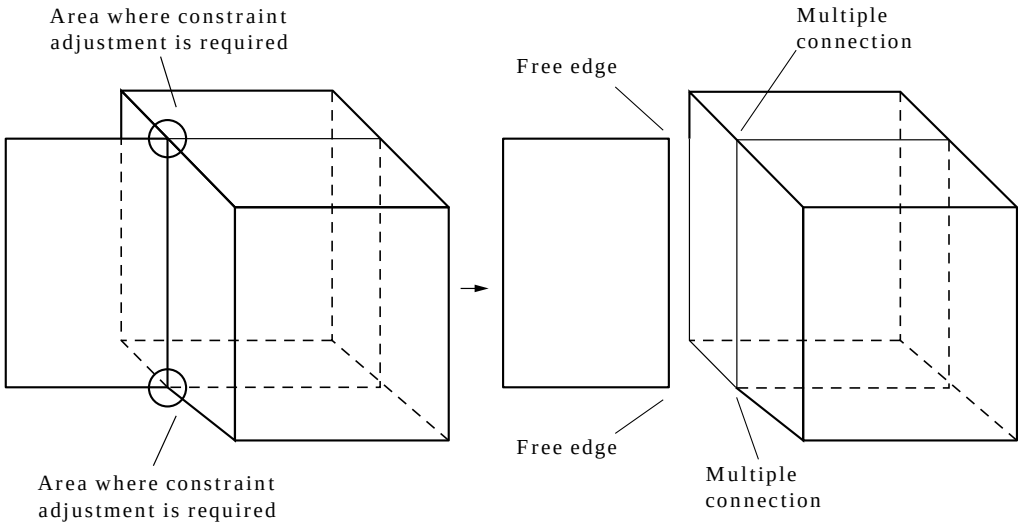

Figure 4. Locations where constraints must be adjusted.

scheme. During this process the element connectivity and the constraint definitions are updated accordingly.

The nodes where the free edge constraints have been assigned are inspected in order to determine the locations where corrective action is required. In a boundary element model of complex geometry, the location where a thin attachment is connected to the remaining object requires special attention. A free edge constraint must be assigned to the node associated with the element of the free edge. However, the remaining elements which correspond to the continuous part of the model must be disassociated from the free edge constraint, otherwise an artificial opening would be introduced in the model. In addition, a multiple connection constraint might be required if multiple elements are connected at that particular location. In order to identify the locations where the constraint definitions must be adapted, the elements attached to the free edge constraints are inspected. Corrective action is required only if an element edge is comprised of a node with a free edge constraint at one end and a node with a multiple connection constraint at the other. This criterion is utilized to identify all the locations where a thin section is attached to the main object.

Modification of constraint definitions for locations identified during the previous step. Extra nodes are generated for the previously identified locations. One additional node is generated for each element corresponding to the thin section at the connection. There is no limitation on the number of thin sections attached to the main object. The free edge constraints are assigned to all the new nodes attached to the thin sections. At the same time they are removed from the nodes attached to the elements corresponding to the main object. The latter are finally inspected to determine whether a multiple connection constraint must be defined for them or not. Figure 4 demonstrates a simple geometry where this constraint modification is necessary.

Information transfer. Finally the updated boundary element model, including the new nodes along the multiple connections, is utilized for the indirect boundary element analysis. The node numbers associated with the free edges identify the locations in the system matrix where the penalty terms must be added. The multiple connection constraints, identified in terms of nodes involved in them, and the directional coefficients, determine the locations

where the extra terms will be added in the system matrix in order to account for the constraint equations.

This summarizes the algorithm developed for the automated identification and generation of the constraint equations. As it can be deducted, for a practical application this process can be very tedious if attempted to be completed manually. Therefore, for the development of the algorithm presented here and its implementation, software is essential for solving any application with complex geometry using the IBEM.

5. VERIFICATION

The validation of the multiple and free edge constraints development was performed in three steps: (1) validation of the algorithm which generates the constraints; (2) validation of numerical implementation by comparison to an analytical solution, and an other alternative multizone numerical solution; (3) comparison between numerical results and test data.

First the algorithm which generates the constraints was verified. This was achieved by creating the constraints for a series of boundary element models with complex geometry (Figure 5). The generation of the constraints was validated by: (1) verifying that constraints existed in the expected locations; (2) identifying that the boundary element model was modified accordingly; (3) inspecting that the directional coefficients were assigned properly.

The numerical implementation of the constraint equations was verified by comparing the numerical results to an analytical solution for a transversely oscillating rigid disk [19] and by comparing the results obtained by this developement to a multi-zone direct boundary element solution for the complex geometry of a silencer configuration.

An analytical solution for the radiated field generated by a freely vibrating rigid disk [19] was utilized for an initial validation. The boundary element model for the disk is depicted in Figure 6. The transmission coefficient D_1 is defined in reference [19] as

$$D_1 = \frac{W_1 2k}{\pi v^2 \rho \omega}, \tag{18}$$

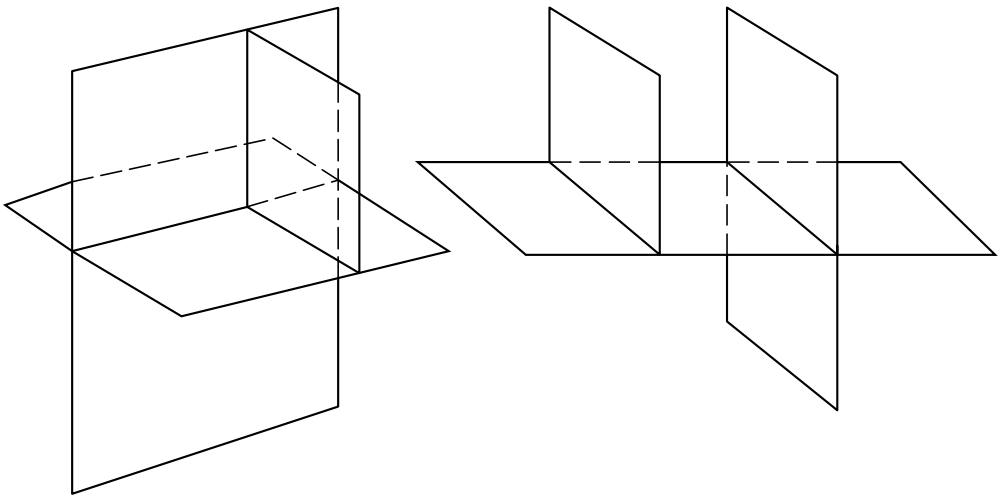

Figure 5. Typical configurations utilized in testing the constraint generation algorithm.

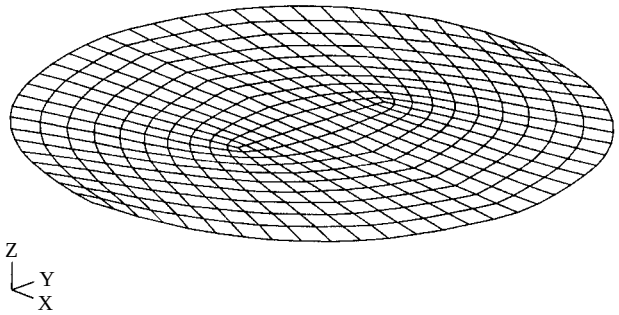

Figure 6. Boundary element model of rigid disk.

where k is the wavenumber, v is the amplitude of oscillation velocity, ω is the radial velocity, and W_1, the radiated power, was computed. Results for wavenumbers from 0 to 8 are presented in Figure 7. The numerical results produced in this development are identical with the analytical results presented in Figure 4 of reference [19].

The complex geometry of a silencer including an internal baffle and an internal cylindrical passage positioned in the middle of the baffle (Figure 8) was utilized for further validation. Two completely different analyses methods were utilized to perform a frequency sweep. The results obtained from this development based on the indirect method were compared to results computed by a multi-zone direct boundary element analysis [20]. The configuration includes interior acoustic cavities connected through a duct extended

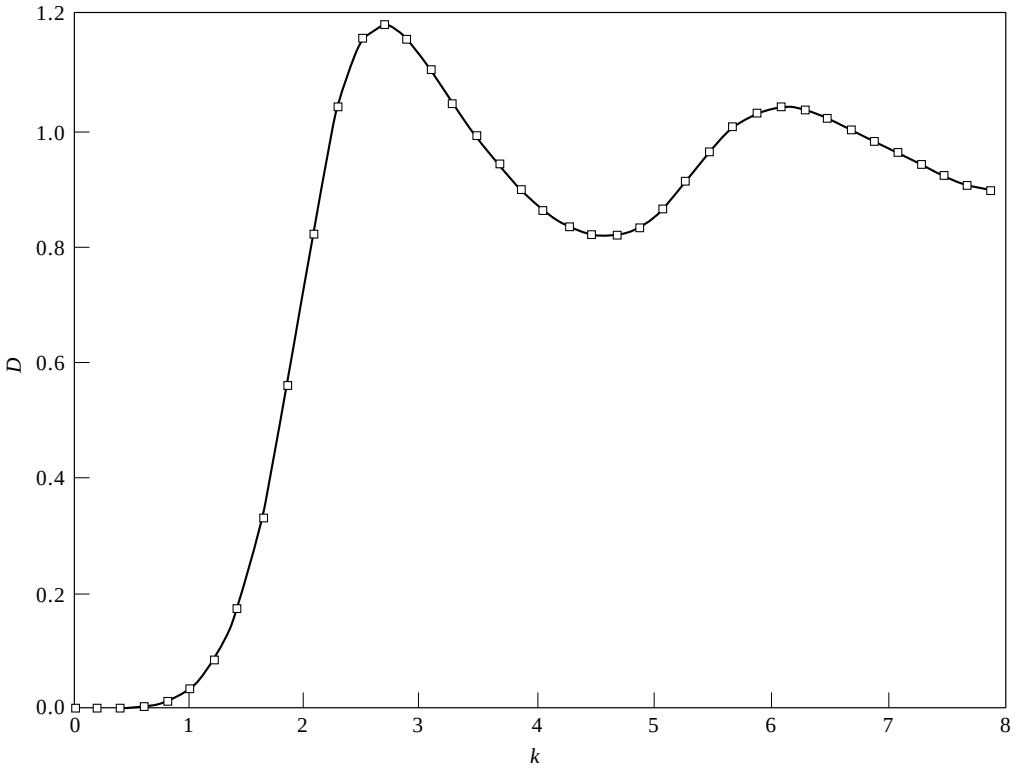

Figure 7. Numerical values for the transmission coefficient of an oscillating rigid disk.

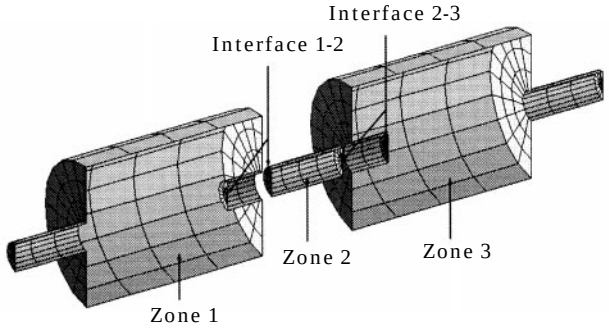

Figure 8. Multi-zone direct boundary element model of silencer.

within each acoustic sub-space. Each cavity is comprised of two cylinders of unequal diameter. This configuration defines a complex geometry. The solution produced by an alternative numerical approach is utilized for validating the development. The indirect model is comprised of a single layer of elements. It includes both free edges and multiple connections. The free edge constraints were assigned at the edges of the inner cylinder connecting the two chambers. The multiple connection constraints were generated for the locations where the inner baffle is attached to the outer shell, and the locations where the baffle is attached to the inner cylinder. In the multi-zone DBEM, the model was divided into three zones (Figure 8). The first and the second chamber were comprising Zones 1 and 3. The middle cylinder is designated as Zone 2. Each zone is defined as a completely enclosed boundary element model. Therefore, overlapping elements exist at the common boundaries between different zones. When the common boundary provides a rigid separation between the two zones (i.e., area defining the baffle between Zone 1 and Zone 3), then the nodes and the elements for each zone are completely separate. At an open connection between two zones (i.e., area of the opening between Zone 1 and Zone 2 at the opening of the inner cylinder), the nodes are shared between the adjacent zones. In the analyses, a unit velocity boundary condition was defined as excitation at the inlet of the system, while an anechoic termination boundary condition was defined at the outlet. Results were computed for the frequency range 100–400 Hz. The results for the acoustic pressure at four internal points were compared between the two methods (Figures 6(a) and (b)). Two data recovery points were located within Zone 1 (first chamber), and the other two in Zone 3 (second chamber). Each one of the two points within each zone was located at an off-center position. Results from the two boundary element methods for the two points located in Zone 1 are presented in Figure 9(a). Similar results for the points located in Zone 3 are presented in Figure 9(b). There is good agreement of the results produced by the two different numerical methods. This validates the mathematical formulation and numerical implementation of the free edge and the multiple connection constraints, since it compares results produced by a model including constraints, with results computed by a completely different numerical method (multi-zone DBEM).

Finally, test results for the noise radiated from a thin corrugated vibrating plate (Figure 10) were compared to numerical results computed by the IBEM. In this application, noise is emitted from both sides of the plate. The model contained 1840 elements and 1920 nodes. It also included 150 free edge constraints. The excitation from a shaker was applied at an off-center location at 942 Hz. The vibration was measured by a laser holography technique. It comprised the excitation boundary conditions for the acoustic analysis. A data recovery plane (array of microphones) was defined 286 mm away from the vibrating plate. Results

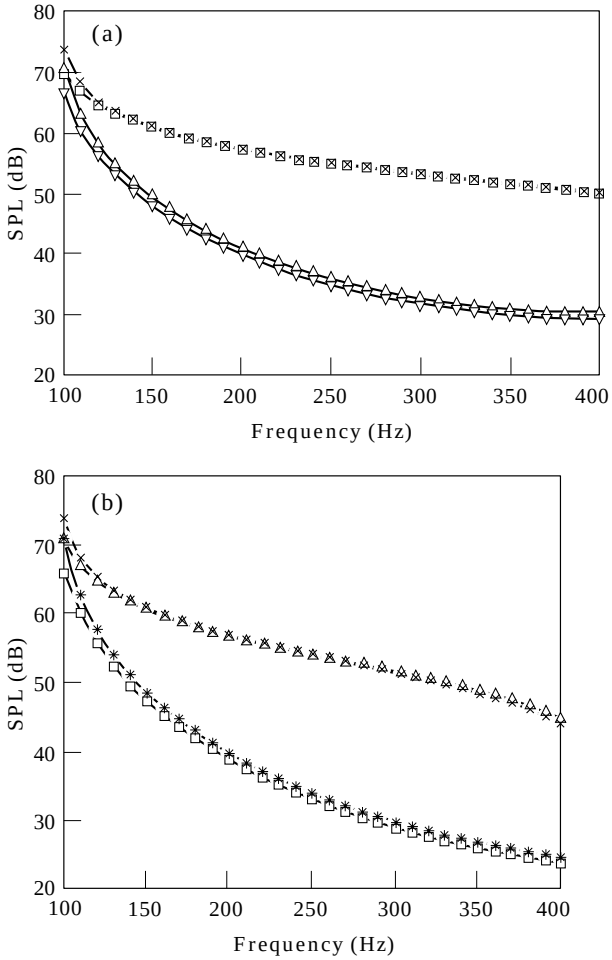

Figure 9. Comparison between DBEM and IBEM for (a) points 1 and 2 (□, DBEM-Point 1; ×, IBEM-Point 2; ▽,DBEM-Point 2; ▼, IBEM-Point 2); (b) Points 3 and 4. (△, DBEM–Point 3; □, DBEM–Point 4; ×, IBEM–Point 3; ✱, IBEM–Point 4).

from the numerical analysis for the sound pressure level are presented in Figure 8. For nine points (highlighted in Figure 11) the computed results are compared successfully to test data collected during the test. Table 1 summarizes the results. Very good agreement between numerical results and test data can be observed. This application offers another validation of the formulation and implementation of the constraints in the IBEM.

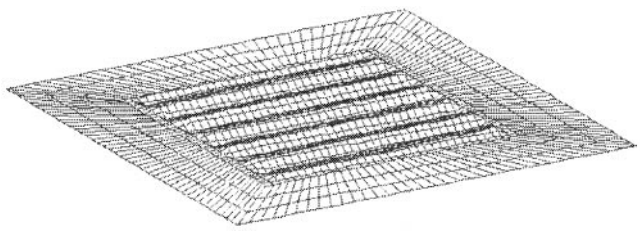

Figure 10. Acoustic indirect boundary element model of thin corrugated plate.

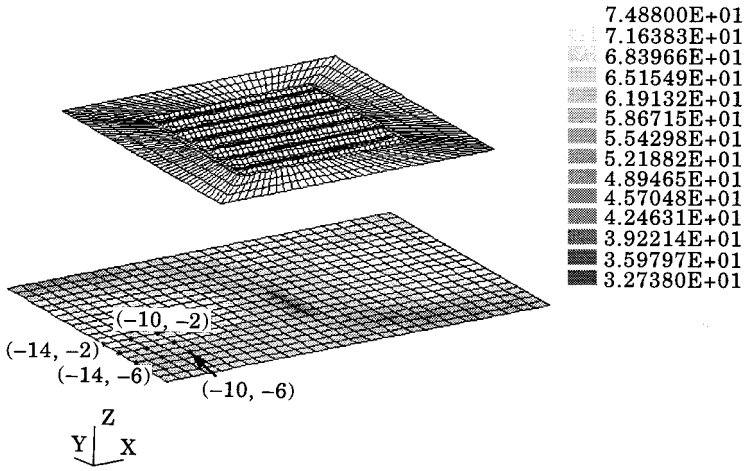

Figure 11. Sound pressure level distribution (dB) on data recover surface (frequency 942·00 Hz).

6. CONCLUSIONS

Multiple connections and free edges can be encountered in boundary element models with complex geometries. In this paper the following new developments are presented: (1) a mathematical formulation of constraints representing free edges and multiple connections; (2) a numerical implementation of the constraints in an indirect boundary element scheme; (3) an algorithm for the automated identification and generation of the constraints.

All the new developments were verified through a series of validations. First the automated generation of the constraints was verified by inspecting the locations and the constraint equations defined for a series of complex geometries. Then numerical results from indirect boundary element applications which included constraints were compared to numerical results produced by the direct multi-zone boundary element method and to an analytical solution. Finally, test data were successfully compared to numerical results for noise radiated from a corrugated thin plate. The capability developed in this work is necessary in order to utilize the indirect boundary element method in computing the noise generated from the vibration of complex structures.

TABLE 1

Comparison of SPL between numerical results and test data for noise radiated from a corrugated plate

Point no.	Measured SPL	Computed SPL
1	71·0	71·6
2	70·50	70·8
3	69·4	69·6
4	67·0	68·4
5	67·0	67·8
6	67·0	67·0
7	58·5	64·4
8	61·0	64·0
9	62·0	63·4

ACKNOWLEDGMENT

This work was partially sponsored by the Automated Analysis Corporation under contract number 970274.

REFERENCES

1. R. D. Cickowski and C. A. Brebbia (editors) 1991 *Boundary Element Methods in Acoustics*. Southampton, Boston: Computational Mechanics Publications; and London, New York: Elsevier Applied Science.
2. G. Chertock 1964 *Journal of the Acoustical Society of America* **36**, 1305–1313. Sound radiation from vibrating surfaces.
3. A. F. Seybert, B. Soenarco, F. J. Rizzo and D. J. Shippy 1984 *Journal of Vibration, Acoustics, Stress, and Reliability in Design* **106**, 414–419. Application of the BIE method to sound radiation problems using an isoparametric element.
4. D. C. Smith 1988 *Ms Thesis, Purdue University*. Noise control design of vibrating structures using the boundary element method.
5. M. A. Hamdi and J. M. Ville 1986 *Journal of Sound and Vibration* **107**, 231–242. Sound radiation from ducts: theory and experiment.
6. J. P. Coyette and K. R. Fyfe 1989 *Proceedings, Numerical Techniques in Acoustic Radiation, Winter Annual Meeting of ASME, San Francisco, CA*, 15–25. Solution of elasto-acoustic problems using a variational finite element/boundary element technique.
7. C. Vallance and N. Vlahopoulos 1996 *Sound and Vibration*, April, 30–34. The prediction of structural noise induced vibration.
8. S. G. Mikhlin 1964 *Variational Methods in Mathematical Physics*. New York: MacMillan.
9. S. M. Kirpur and R. J. Tyrrell 1992 *International Journal of Vehicle Design* **13**, 388–402. Computer-aided analysis of engine noise.
10. M. Hazel, C. Norrey, H. Kikuchi and D. Tres 1996 *Proceedings of International Congress and Exposition, Detroit, MI, SAE Paper No*. 960145. Using predictive acoustic analysis to evaluate noise issues in under hood applications.
11. T. C. Tecco, N. Vlahopoulos and E. J. Vorenkamp 1993 *International Off-Highway & Powerplant Congress & Exposition, Milwaukee, WI, SAE Paper No*. 932433. Application of numerical acoustics methods to noise reduction in vehicle compartments.
12. N. Vlahopoulos, E. V. Shalis and M. A. Latcha 1993 *Proceedings* 14*th ASME Biennial Conference on Mechanical Vibration and Noise, Albuquerque, NM*, 73–80. A numerical approach for the prediction and reduction of structure-borne noise during the design stage of ground vehicles.
13. N. Basavanhalli, R. Sommers, L. Brooks, F. Zweng and W. Kargus 1995 *SAE, Proceedings of the Ninth International Conference on Vehicle Structural Mechanics and CAE, SAE Paper No*. 951092. Reduction of passenger car road noise using computational analysis.
14. K. A. Cunefare, G. Koopman and K. Brok 1989 *Journal of the Acoustical Society of America* **85**, 39–47. A boundary element method for acoustic radiation valid for all wavenumbers.
15. H. Lamb 1932 *Hydrodynamics*. New York: Dover: Sixth edition.
16. P. K. Banerjee 1994 *The Boundary Element Methods in Engineering*. New York: McGraw-Hill.
17. S. S. Rao 1989 *The Finite Element Method in Engineering*. Oxford: Pergamon Press: second edition.
18. R. T. Haftka and M. P. Kamat 1985 *Elements of Structural Optimization*. The Hague: Martinus Nijhoff Publishers.
19. C. J. Boukamp 1970 *IEEE Transactions on Antennas and Propagation* **18**, 152–176. Theoretical and numerical treatment of diffraction through a circular aperture.
20. C. Y. R. Cheng 1988 *PhD Dissertation, University of Kentucky*. Boundary element analysis of single and multidomain problems in acoustics.